Electronic Supplementary Material (ESI) for Nanoscale.
This journal is © The Royal Society of Chemistry 2018

Supporting Information

Improved structural design of single- and double-wall $MnCo_2O_4$ nanotube cathodes for long-life Li-O_2 batteries

*Haitao Wu,[a] Wang Sun,[*a,b] Junrong Shen,[a] Chengyi Lu,[a] Yan Wang,[a] Zhenhua Wang[a,c] and Kening Sun[*a,c]*

[a] Beijing Key Laboratory for Chemical Power Source and Green Catalysis, School of Chemistry and Chemical Engineering, Beijing Institute of Technology, Beijing 100081, China.

[b] State Key Laboratory of Advanced Chemical Power Sources, Guizhou Meiling Power Sources Co. Ltd., Zunyi, Guizhou 563003, China

[c] Collaborative Innovation Center of Electric Vehicles in Beijing, No.5 Zhongguancun South Avenue, Haidian District, Beijing 100081, China

Corresponding Authors

[*]E-mail address: sunwang@bit.edu.cn (Wang Sun);

bitkeningsun@163.com (Kening Sun).

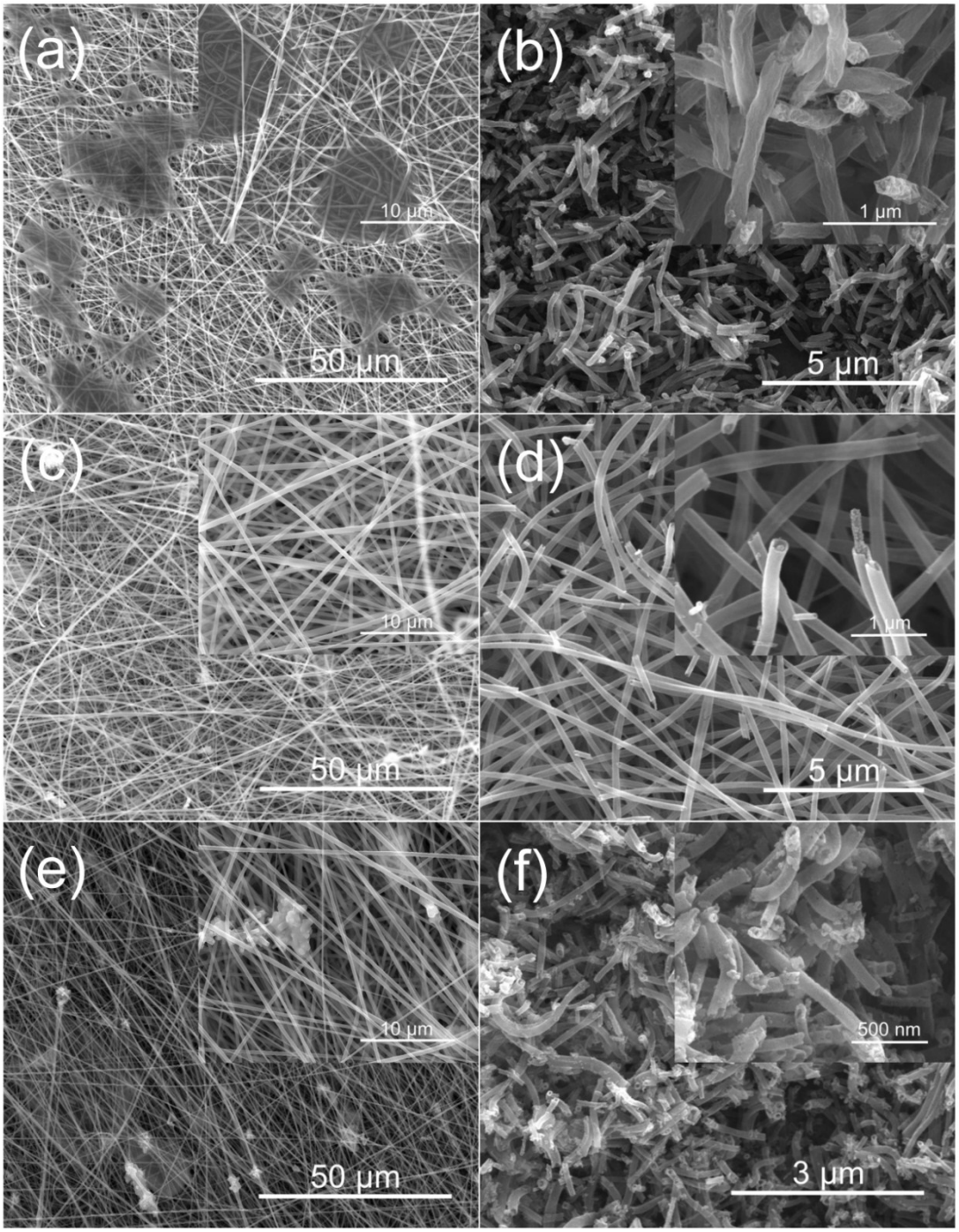

Fig. S1 Low- and high-magnification SEM images of the as-electrospun precursor nanofibers with M:PVP=0.59:1 (a), M:PVP=0.92:1 (b), and M:PVP=1.12:1 (c) before calcination, and the corresponding nanostructures (d), (e), and (f) after calcination in air, respectively.

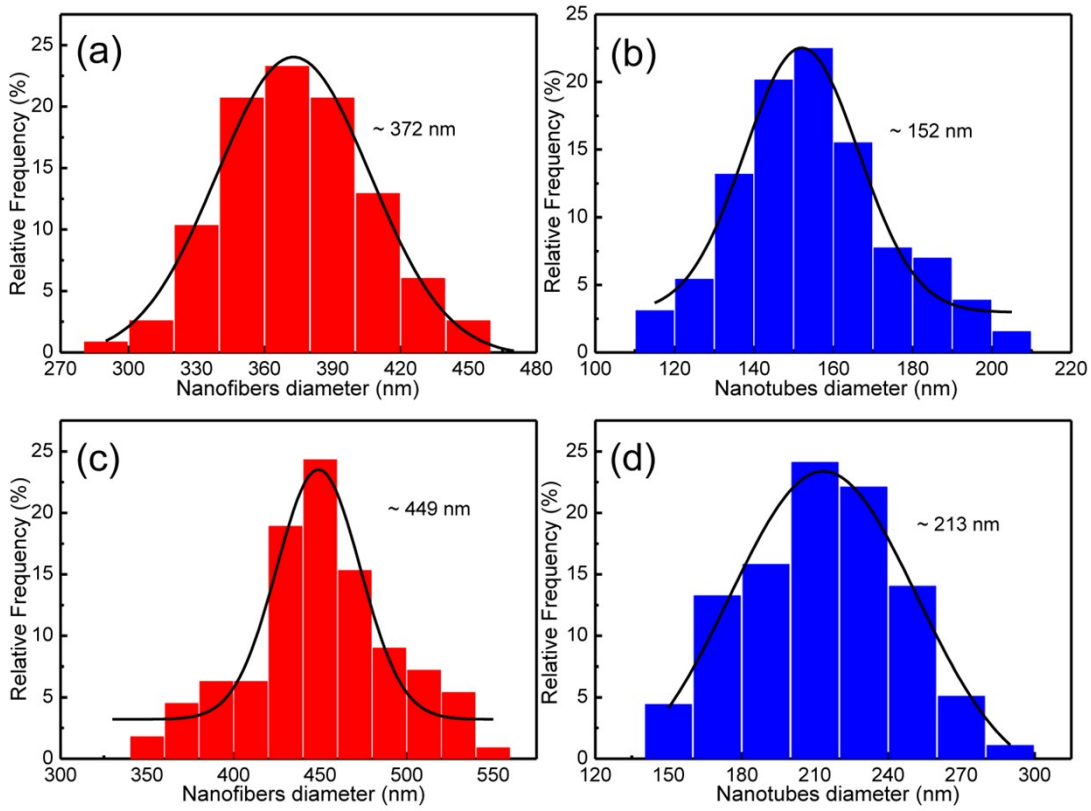

Fig. S2 Diameter distribution histograms of the as-electrospun nanofibers with M:PVP=1.01:1 (a) and M:PVP=0.74:1 (c) before calcination, and the corresponding SW-MCO-NT (b) and DW-MCO-NT (d) after calcination in air, respectively.

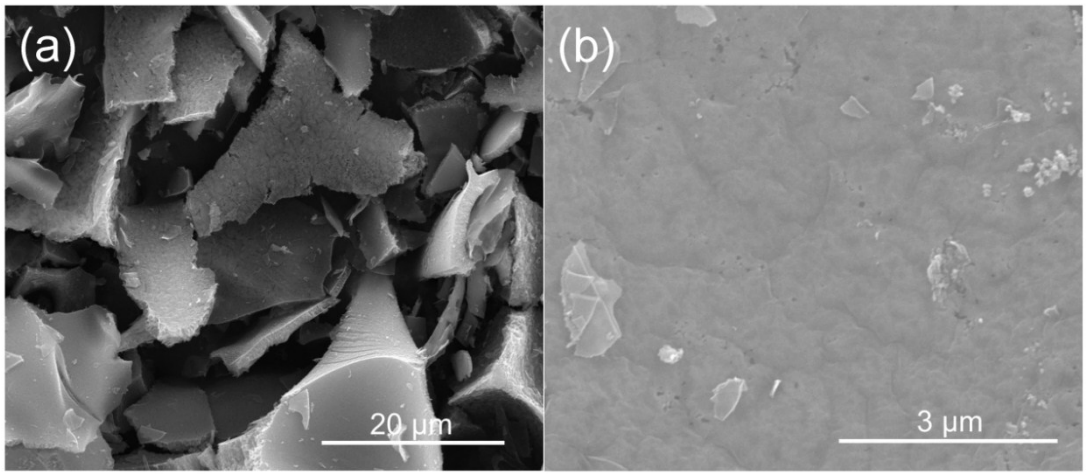

Fig. S3 SEM images of the B-MCO synthesized by a sol-gel method.

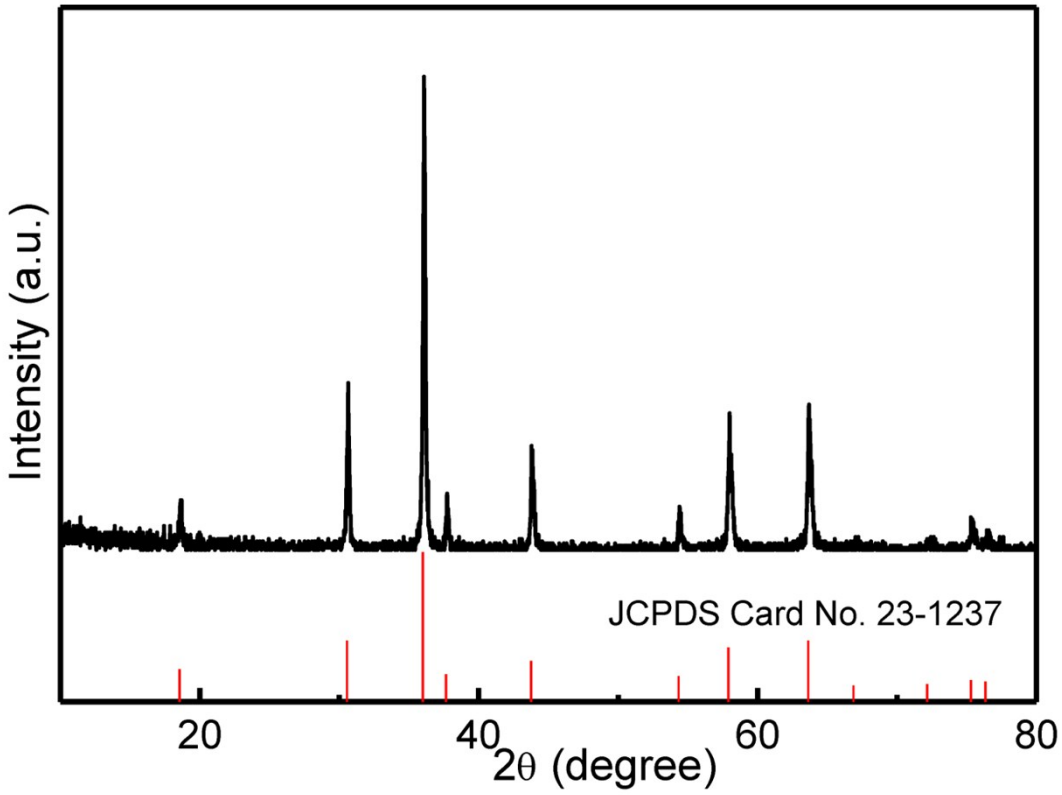

Fig. S4 XRD patterns of the B-MCO sample.

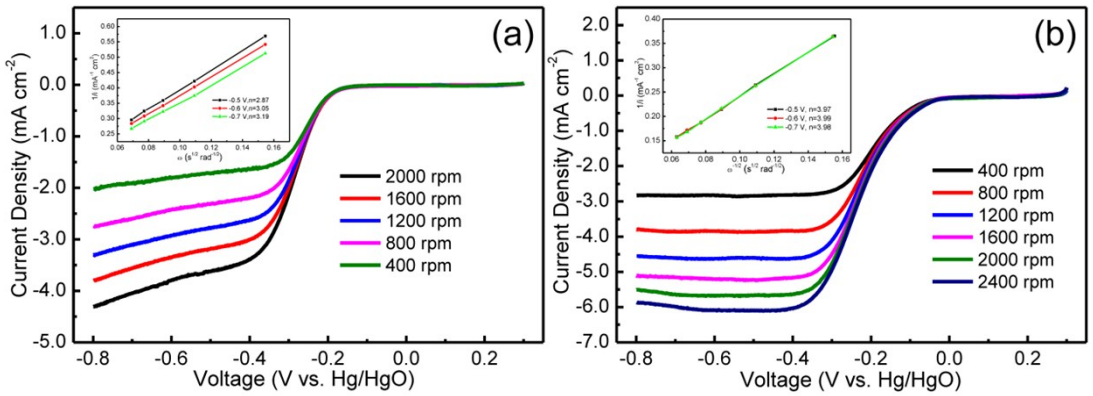

Fig. S5 Rotating disk voltammograms of B-MCO (a) and SW-MCO-NT (b) under different rotating speeds, and corresponding K-L plots at different potentials (inset).

Table S1. Comparison of the CV, ORR, and OER of the $MnCo_2O_4$ samples, commercial Pt/C and RuO_2 catalysts in alkaline solution.

Catalyst	CV		ORR		OER	
	E_{peak} (V)	I_{peak} (mA cm^{-2})	E_{onset} (V)	$I_{limiting}$ (mA cm^{-2})	$E_{half\text{-}wave}$ (V)	I_{max} (mA cm^{-2})
Pt/C	-	-	0.021	–5.50	-	-
DW-MCO-NT	–0.134	–0.53	0.020	–5.12	0.830	23.56
SW-MCO-NT	–0.153	–0.47	–0.019	–5.11	0.846	21.75
B-MCO	–0.201	–0.21	–0.156	–3.76	-	6.65
RuO_2	-	-	-	-	0.794	22.80

E_{onset} (V) at I=–0.07 mA cm^{-2}

$I_{limiting}$ at E=–0.8 V

I_{max} at E=1.0 V

$E_{half\text{-}wave}$ (V) at I=10 mA cm^{-2}

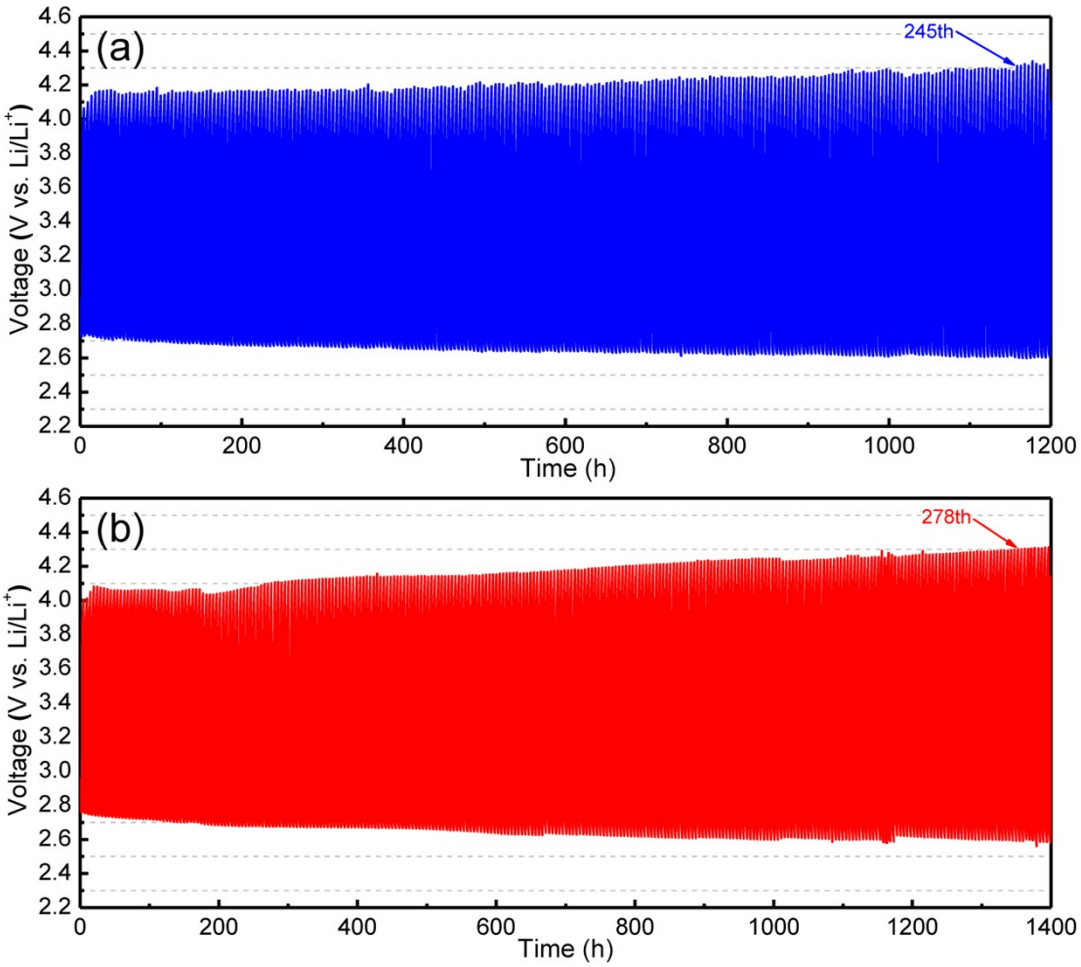

Fig. S6 Discharge/charge voltage profiles of the (a) SW-MCO-NT and (b) DW-MCO-NT electrode with a capacity limitation of 1000 mAh g^{-1} at 400 mA g^{-1} within 2.6–4.3 V.

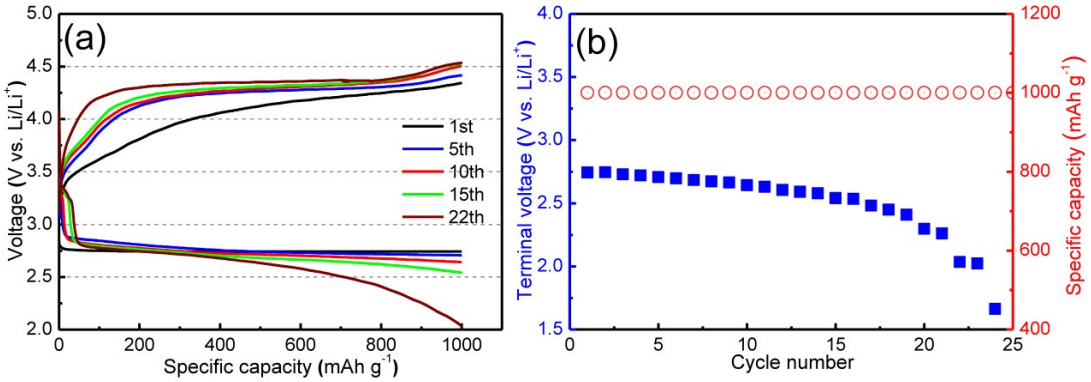

Fig. S7 (a) Discharge/charge curves of the Li-O_2 cell with the B-MCO electrode with a capacity limitation of 1000 mAh g^{-1} at 400 mA g^{-1}. (b) The corresponding terminal discharge voltage vs. the cycle number.

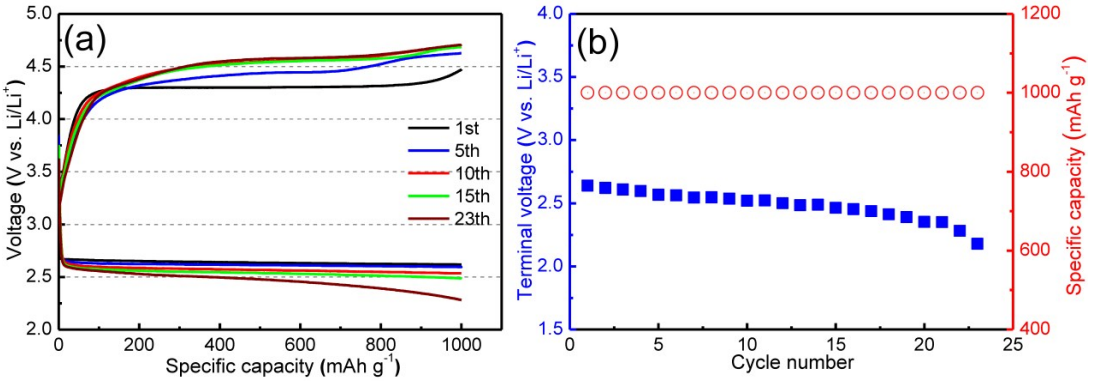

Fig. S8 (a) Discharge/charge curves of the Li-O_2 cell with the pure Super P based electrode under a limited capacity of 1000 mAh g^{-1} at 400 mA g^{-1}. (b) The corresponding terminal discharge voltage vs. the cycle number.

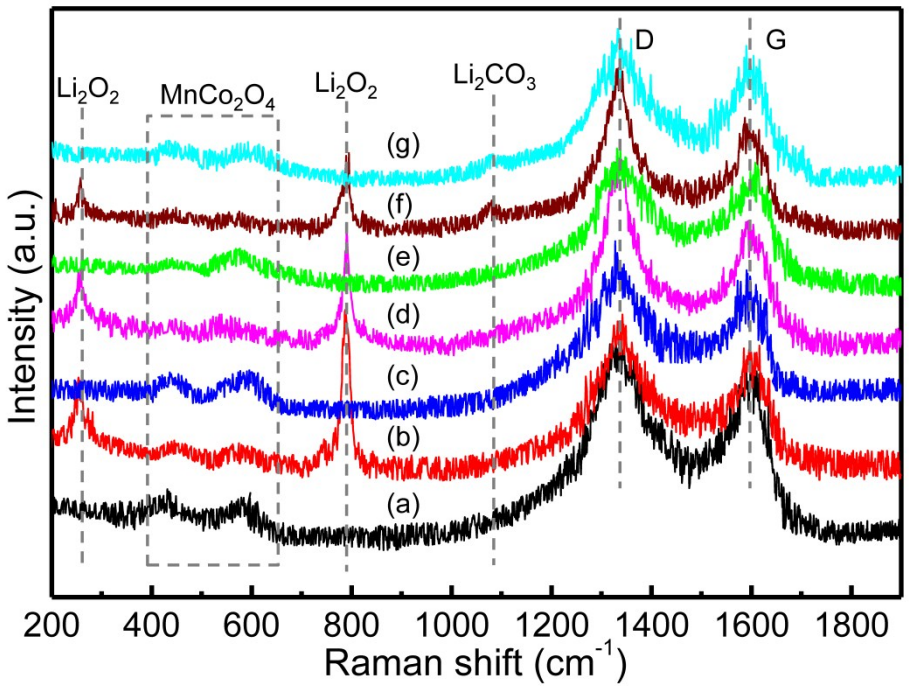

Fig. S9 Raman spectra of the DW-MCO-NT electrode: pristine electrode (a), 1st discharge (b), 1st charge (c), 100th discharge (d), 100th charge (e), 230th discharge (f), and 230th charge (g).

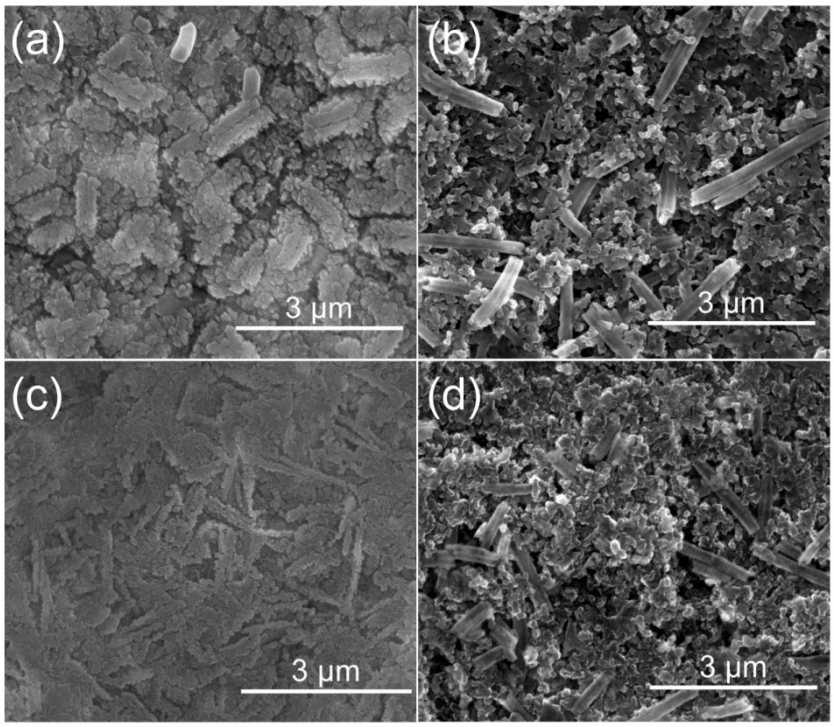

Fig. S10 SEM images of the DW-MCO-NT electrode after 100th discharge (a), 100th recharge (b), 230th discharge (c), and 230th recharged (d).

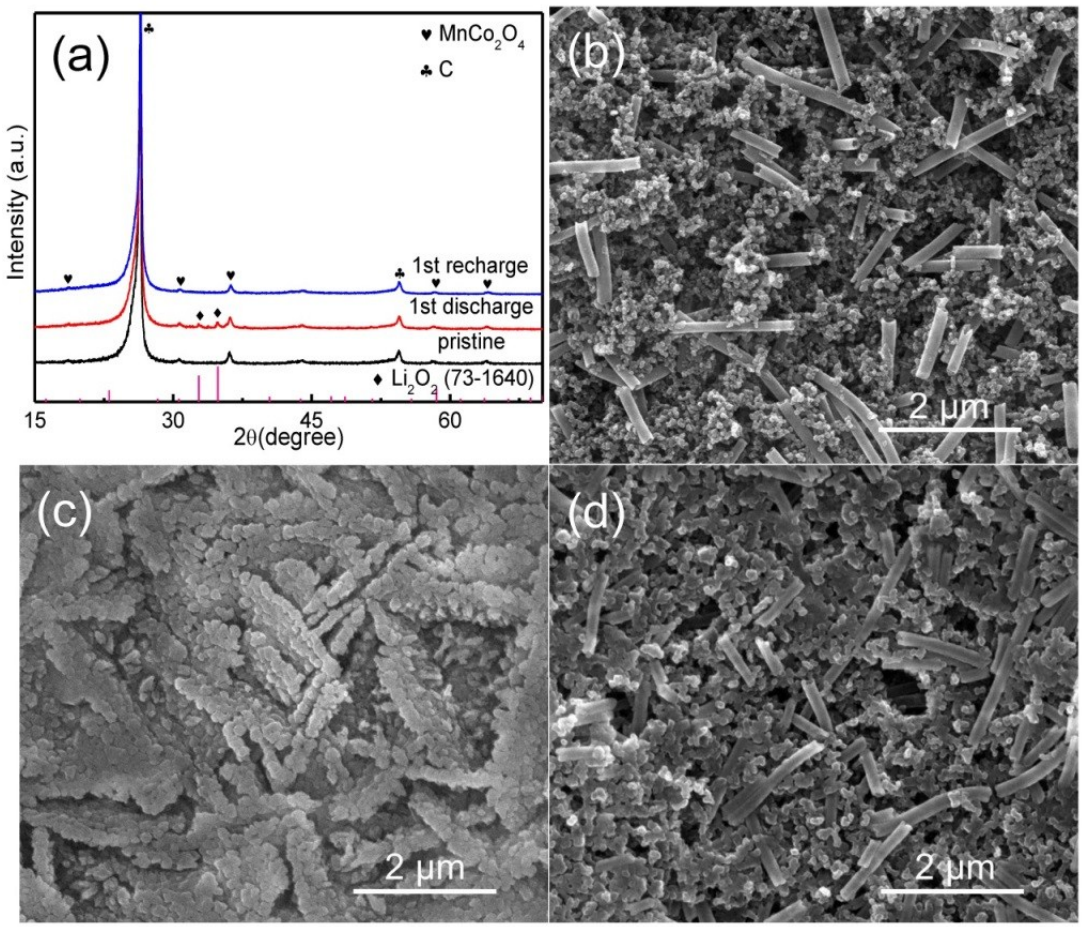

Fig. S11 (a) XRD patterns of the SW-MCO-NT electrode at different discharge/charge states. SEM images of the SW-MCO-NT electrode before discharge (b), after 1st discharge (c), and 1st recharged (d).

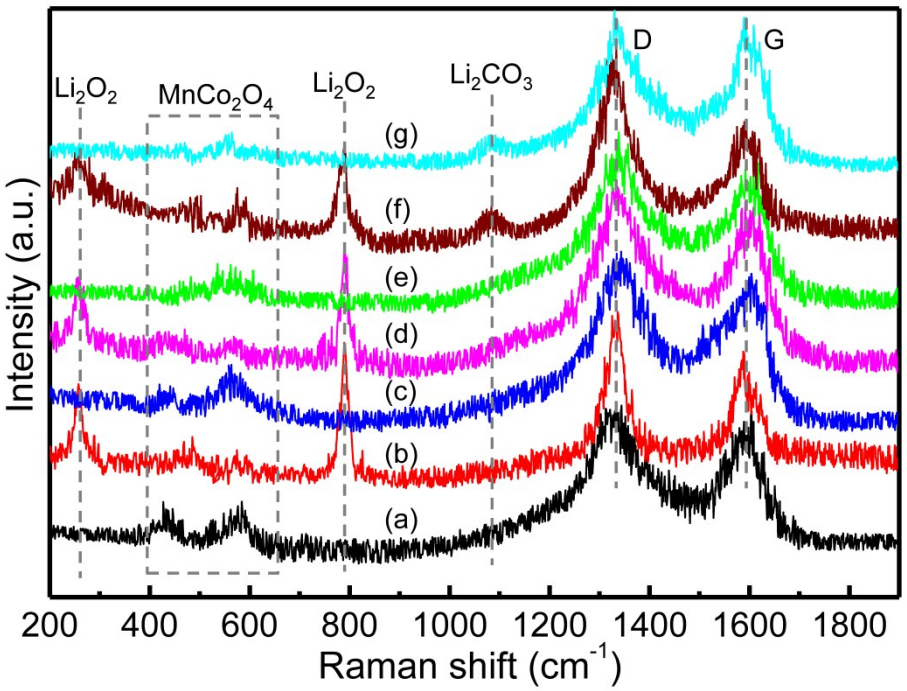

Fig. S12 Raman spectra of the SW-MCO-NT electrode: pristine electrode (a), 1st discharge (b), 1st charge (c), 100th discharge (d), 100th charge (e), 230th discharge (f), and 230th charge (g).

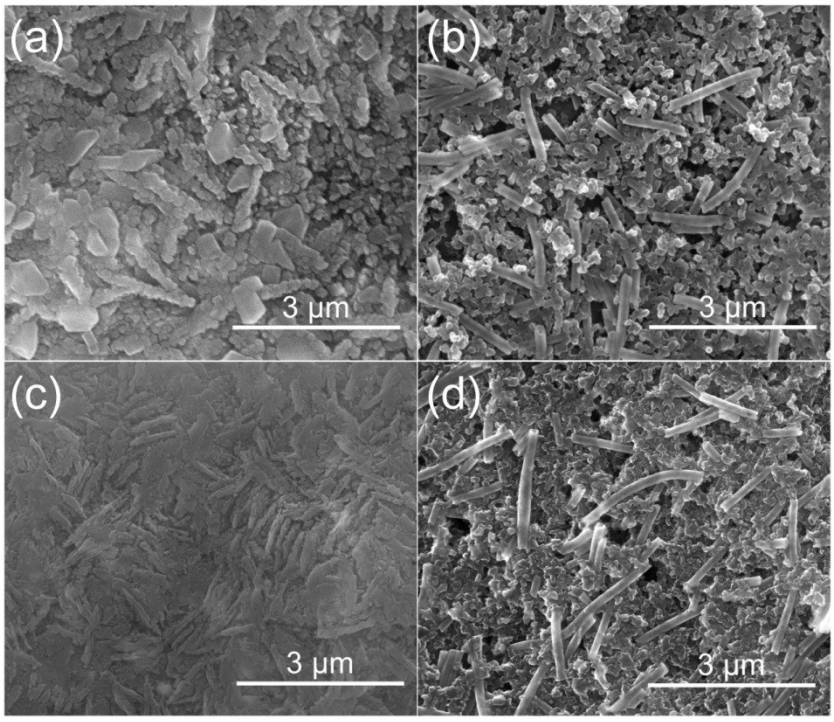

Fig. S13 SEM images of the SW-MCO-NT electrode after 100th discharge (a), 100th recharge (b), 230th discharge (c), and 230th recharged (d).

Table S2. Summary of electrochemical performances of Li-O_2 batteries with transition-metal oxides based catalysts.

Catalyst	Maximum capacity (current density)	Cycle (upper-limited capacity, current density)	Cyclic cut-off voltage	Electrolyte	Ref.
RuO_2@ $La_{0.6}Sr_{0.4}Co_{0.8}Mn_{0.2}O_3$ nanofibers	12742 mAh g^{-1} (50 mA g^{-1})	100 (500 mAh g^{-1}, 50 mA g^{-1})	~2.6–4.3 V	1 M LiTFSI /TEGDME	[1]
$NiCo_2O_4$@Co_3O_4 hybrid	4386 mAh g^{-1} (100 mA g^{-1})	60 (500 mAh g^{-1}, 100 mA g^{-1})	~2.0–4.3 V	1 M LiTFSI /TEGDME	[2]
$NiMn_2O_4$-FT particles	9440 mAh g^{-1} (150 mA g^{-1})	50 (900 mAh g^{-1}, 150 mA g^{-1})	~2.0–4.5 V	1 M LiTFSI /TEGDME	[3]
Yolk-shell Co_2CrO_4 nanospheres	6260 mAh g^{-1} (200 mA g^{-1})	236 (1000 mAh g^{-1}, 200 mA g^{-1})	~2.0–4.5 V	1 M LiTFSI /TEGDME	[4]
3D ordered macroporous $CoFe_2O_4$	4663 mAh g^{-1} (200 mA g^{-1})	47 (500 mAh g^{-1}, 200 mA g^{-1})	~2.3–4.5 V	1 M LiTFSI /TEGDME	[5]
Yolk-shell Co_3O_4@Co_3O_4 /Ag	12000 mAh g^{-1} (200 mA g^{-1})	80 (1000 mAh g^{-1}, 200 mA g^{-1})	~2.3–4.5 V	1 M LiTFSI /TEGDME	[6]
MnCoO-CNT composite microspheres	37142 mAh g^{-1} (200 mA g^{-1})	245 (500 mAh g^{-1}, 200 mA g^{-1})	~2.0–4.35 V	Mixture[a]	[7]
$NiFe_2O_4$/C nanofibers	5.5 mAh (0.1 mA cm^{-2})	40 (0.5 mAh, 0.1 mA cm^{-2})	~2.4–4.5 V	1 M LiTFSI /TEGDME	[8]
$MnCo_2O_4$-graphene hybrid	3784 mAh g^{-1} (100 mA g^{-1})	40 (1000 mAh g^{-1}, 100 mA g^{-1})	~2.5–4.3 V	1 M $LiClO_4$ /PC	[9]
$MnCo_2O_4$ Microspheres	4861 mAh g^{-1} (200 mA g^{-1})	50 (1000 mAh g^{-1}, 250 mA g^{-1})	~2.5–4.4 V	1 M LiTFSI /TEGDME	[10]

Bio $MnCo_2O_4$ nanowires	7076 mAh g^{-1} (~220 mA g^{-1})	16 (200 mAh g^{-1}, 100 mA g^{-1})	~2.0–4.3 V	0.1 M $LiClO_4$ /DME	[11]
$MnCo_2O_4$ nanowires /RGO	11092.1 mAh g^{-1} (200 mA g^{-1})	35 (1000 mAh g^{-1}, 200 mA g^{-1})	~2.3–4.3 V	1 M $LiPF_6$ /TEGDME	[12]
$MnCo_2O_4$/ P-doped porous carbon	13150 mAh g^{-1} (200 mA g^{-1})	200 (1000 mAh g^{-1}, 200 mA g^{-1})	~2.6–4.4 V	1 M LiTFSI /TEGDME	[13]
$MnCo_2O_4$ hollow nanocages	2050 mAh g^{-1} (50 mA g^{-1})	70 (600 mAh g^{-1}, 400 mA g^{-1})	~2.1–4.5 V	1 M LiTFSI /TEGDME	[14]
$MnCo_2O_4$ nanowire bundles/ Ni foam	12919 mAh g^{-1} (0.1 mA cm^{-2})	144 (1000 mAh g^{-1}, 0.1 mA cm^{-2})	~2.2–4.4 V	1 M $LiClO_4$ /DMSO	[15]
$MnCo_2O_4$ nanorods /Ni foam	10520 mAh g^{-1} (100 mA g^{-1})	119 (1000 mAh g^{-1}, 500 mA g^{-1})	~2.0–4.2 V	1 M LiTFSI /TEGDME	[16]
SW-MCO-NT	6360 mAh g^{-1} (200 mA g^{-1})	245 (1000 mAh g^{-1}, 400 mA g^{-1})	~2.6–4.3 V	1 M LiTFSI /TEGDME	This work
DW-MCO-NT	7501 mAh g^{-1} (200 mA g^{-1})	278 (1000 mAh g^{-1}, 400 mA g^{-1})	~2.6–4.3 V	1 M LiTFSI /TEGDME	This work

Mixture[a]: 0.5 M LiTFSI, 0.5 M $LiNO_3$, and 0.05 M LiI /TEGDME.

References

1 X. Zhang, Y. Gong, S. Li and C. Sun, *ACS Catal.*, 2017, **7**, 7737-7747.

2 P. Sennu, H. S. Park, K. U. Park, V. Aravindan, K. S. Nahm and Y.-S. Lee, *J. Catal.*, 2017, **349**, 175-182.

3 S. Li, J. Xu, Z. Ma, S. Zhang, X. Wen, X. Yu, J. Yang, Z. F. Ma and X. Yuan, *Chem. Commun.*, 2017, **53**, 8164.

4 Q. Zhao, C. Wu, L. Cong, Y. Zhang, G. Sun, H. Xie, L. Sun and J. Liu, *J. Mater. Chem. A*, 2017, **5**, 544-553.

5 J. G. Kim, Y. Noh, Y. Kim, S. Lee and W. B. Kim, *Nanoscale*, 2017, **9**, 5119-5128.

6 R. Gao, Z. Yang, L. Zheng, L. Gu, L. Liu, Y. Lee, Z. Hu and X. Liu, *ACS Catal.*, 2018, **8**, 1955-1963.

7 J. H. Kim, Y. J. Oh and Y. C. Kang, *Carbon*, 2018, **128**, 125-133.

8 X. Zhang, C. Wang, Y.-N. Chen, X.-G. Wang, Z. Xie and Z. Zhou, *J. Power Sources*, 2018, **377**, 136-141.

9 H. Wang, Y. Yang, Y. Liang, G. Zheng, Y. Li, Y. Cui and H. Dai, *Energy Environ. Sci.*, 2012, **5**, 7931.

10 S. Ma, L. Sun, L. Cong, X. Gao, C. Yao, X. Guo, L. Tai, P. Mei, Y. Zeng, H. Xie and R. Wang, *J. Phys. Chem. C*, 2013, **117**, 25890-25897.

11 D. Oh, J. Qi, B. Han, G. Zhang, T. J. Carney, J. Ohmura, Y. Zhang, Y. Shao-Horn and A. M. Belcher, *Nano Lett.*, 2014, **14**, 4837-4845.

12 J. G. Kim, Y. Kim, Y. Noh and W. B. Kim, *ChemSusChem*, 2015, **8**, 1752-1760.

13 X. Cao, J. Wu, C. Jin, J. Tian, P. Strasser and R. Yang, *ACS Catal.*, 2015, **5**, 4890-4896.

14 Y. L. Cao, F. C. Lv, S. C. Yu, J. Xu, X. Yang and Z. G. Lu, *Nanotechnology*, 2016, **27**, 135703.

15 H. Wu, W. Sun, Y. Wang, F. Wang, J. Liu, X. Yue, Z. Wang, J. Qiao, D. W. Rooney and K. Sun, *ACS Appl. Mater. Interfaces*, 2017, **9**, 12355-12365.

16 R. S. Kalubarme, H. S. Jadhav, D. T. Ngo, G. E. Park, J. G. Fisher, Y. I. Choi, W. H. Ryu and C. J. Park, *Sci. Rep.*, 2015, **5**, 13266.